

Prestressed Loss and Deflection of Precast Concrete Members



Maher K. Tadros

Associate Professor
Department of Civil
Engineering
University of Nebraska
Omaha, Nebraska



Amin Ghali

Professor
Department of Civil
Engineering
University of Calgary
Calgary, Alberta, Canada



Arthur W. Meyer

PhD Candidate and PE
Department of Civil
Engineering
University of Nebraska
Omaha, Nebraska

Serviceability, particularly deflection, is today becoming a more important criterion than in the past due to the utilization of modern design procedures and the use of high strength materials which result in slender members more susceptible to large deflections. This is especially true in prestressed concrete applications, particularly when members are allowed to develop cracks under service loads. Cracking could cause a sizable drop in member stiffness and increased deflections.

It is difficult to calculate member deflections with a high degree of accuracy even in a controlled testing laboratory. This is due to the random variations of some of the contributory factors such as the concrete modulus of elasticity, creep, and shrinkage. In field conditions

not only are the variations greater, but in addition the number of variables increase. Examples are the uncertainties about levels and duration of loading and seasonal weather variations. Calculated deflection should therefore be viewed as an "estimate."

Acceptable deflection analysis should not be highly complicated mathematically, which would give a false impression of exactness, nor should it be oversimplified, which would compound the probable errors resulting from uncertainties in material properties and loading variations.

In this paper a simplified approach to computing instantaneous and long-term deflections is proposed. The approach rationally accounts for all the important parameters, yet it involves certain ap-

proximations which make it suitable for manual computations.

Long-term deflection multipliers based on the Trost-Bazant^{1,2} aging coefficient are proposed. These multipliers, unlike those in the current PCI Design Handbook, are shown to be valid for various environmental conditions and when nonprestressed steel is present.

Because prestressing produces deflections that are opposite to and often of the same order of magnitude as the dead loads, it is important to determine precise values of the prestressing force. Further, the presence of nonprestressed steel tends to restrain creep and shrinkage of concrete, and its effect must be included when computing the compression prestress force in concrete.

Since an accurate computation of prestress losses is necessary, a method is presented here for their calculation. It involves a simplification over existing methods that account for environmental variations and for the presence of nonprestressed steel. It is important to note, however, that the proposed deflection procedure itself is independent of the method of prestress loss calculation, and other loss estimates may be used if the designer so desires.

The deflection procedure described herein accounts for possible live load cracking. Two charts are presented for rapid evaluation of the cracked section moment of inertia and centroidal depth. The charts include the effect which axial force and the presence of nonprestressed steel have in increasing the cracked member stiffness. Their use thus results in avoiding unnecessary overestimation of live load deflection.

The live load deflection prediction may further be refined by inclusion of the stiffening effects of uncracked concrete in the tension zone, the so-called "tension stiffening." Tension stiffening is generally accounted for empirically. Formulas are presented here for adjustment of the cracked section moment of inertia and centroidal depth. The Euro-

Synopsis

This paper discusses the influence of creep and shrinkage of concrete, relaxation of prestressed steel, and presence of nonprestressed steel on time-dependent deflection behavior of prestressed concrete members.

Multipliers are developed for predicting time-dependent deflections. Design aids are presented for determining cracked section properties ignoring concrete in tension. Empirical consideration of the stiffening effects of concrete in the tension zone is discussed.

The above factors are integrated into a simple procedure for deflection prediction which is suggested as a modification to the PCI Design Handbook. Although application of the method to precast concrete construction is emphasized, it is equally applicable to cast-in-place post-tensioned members. Two numerical examples are included to illustrate the application of the proposed design method.

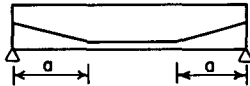
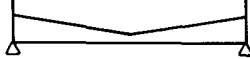
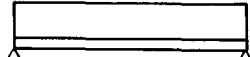
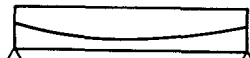
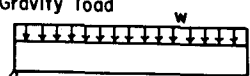
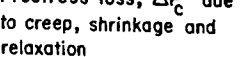
pean Code method (CEB-FIP, 1978), as well as other methods of consideration of tension stiffening, are also discussed.

The proposed method of deflection calculation is verified with test results and compared with other methods, including that in the PCI Design Handbook. Five steps of calculation are proposed and illustrated with numerical examples.

IMMEDIATE DEFLECTION OF UNCRACKED MEMBERS

Immediate deflection, or camber, due to the effects of initial prestressing P_{co} and member self weight is generally calculated by basic principles of mechanics of elastic structures. The value

Table 1. Formula for midspan deflection of uncracked members.

$\delta = \frac{\phi_c l^2}{8} - (\phi_c - \phi_e) (\text{Multiplier})^*$					
		Cause	Midspan Curvature ϕ_c	End Curvature ϕ_e	Multiplier
Immediate deflection	1 †	Two point depressed tendon 	$-\frac{P_{co} e_c}{E_{ci} I_g}$	$-\frac{P_{co} e_e}{E_{ci} I_g}$	$\frac{a^2}{6}$
	2 †	One point depressed tendon 	$-\frac{P_{co} e}{E_{ci} I_g}$	$-\frac{P_{co} e}{E_{ci} I_g}$	$\frac{l^2}{24}$
	3 †	Straight tendon 	$-\frac{P_{co} e_c}{E_{ci} I_g}$	$-\frac{P_{co} e_e}{E_{ci} I_g}$	0
	4 †	Parabolic tendon 	$-\frac{P_{co} e_c}{E_{ci} I_g}$	0	$\frac{l^2}{48}$
	5	Gravity load 	$\frac{w l^2}{8 E_{ci} I_g}$	0	$\frac{l^2}{48}$
Time dependent deflection	6 ‡	Prestress loss, ΔP_c due to creep, shrinkage and relaxation 	$-\frac{\Delta P_c (e_{ts})_c}{E_{ci} I_g} (1 + \chi C_u)$	$-\frac{\Delta P_c (e_{ts})_e}{E_{ci} I_g} (1 + \chi C_u)$	$\frac{l^2}{48}$

* If the two end curvatures are not equal, use an average value of the two curvatures for ϕ_e .

† Eccentricity to be used is that of the prestressing steel.

‡ Eccentricity to be used is that of the total steel. The term $(1 + \chi C_u)$ is valid only for deflection at time infinity; for other multipliers see Table 2.

of P_{co} is equal to the jacking force less the initial prestress loss due to anchorage set, elastic shortening, and relaxation loss occurring between jacking and release time. References 3, 4, and 5 discuss in detail the calculation of P_{co} .

A simplified form of calculating P_{co} is

presented in Appendix A. Curvature at a section is equal to bending moment divided by the section rigidity, EI ; where E = modulus of elasticity of concrete at the time of prestress transfer and I = moment of inertia of the section, which is simple to determine because cracking

is commonly not allowed to occur at this stage.

In most cases, the moment of inertia may be approximately taken equal to that of the gross concrete area, $I = I_g$. If there is an unusually large amount of reinforcing steel present, the accuracy will be improved by use of the properties of the transformed section.

The value of P_{co} includes the compression force picked up by the nonprestressed steel due to elastic shortening at transfer. However, for simplicity the location of P_{co} is assumed to coincide with that of the prestressed steel, rather than the exact location of the resultant of the relatively large tension force in the prestressed steel and the much smaller compression force in the nonprestressed steel.

Standard design aids, such as Fig. 3.9.18 and Fig. 8.1.4 of the PCI Design Handbook,⁴ may be used for calculating the immediate deflection of uncracked members. Table 1 of the present paper includes a deflection formula which, when used for initial prestress camber, should yield identical results to those given in Fig. 3.9.18 of the PCI Design Handbook for straight, single-point depressed, and two-point depressed tendons. The Table 1 formula is also useful for other cases including prestress loss deflection as will be discussed in a separate section.

IMMEDIATE DEFLECTION OF CRACKED MEMBERS

Discussion of the behavior of cracked prestressed members follows.

Cracked Section Properties

Two facts about the geometric properties of cracked prestressed concrete members should be clearly understood.

1. Prestressed concrete flexural members are different from reinforced concrete members in that prestressed

members are simultaneously subject to both axial force and bending moment. The axial force may be sufficiently high to permit no cracks or extremely low that the member behaves as a conventionally reinforced member. Therefore, for a given bending moment at a section, the moment of inertia varies from the gross I to the cracked I of a conventionally reinforced section depending on the magnitude of the prestressing force.

2. Furthermore, the neutral axis which is located at the bottom of the concrete compression zone (assuming positive bending moment), does not coincide with the centroid of the transformed cracked section when an axial force exists. For example, when the axial force combined with the bending moment produce zero stress at the bottom fibers, the neutral axis will be located at the bottom edge of the section while the centroid is, obviously, much higher. The moment of inertia must be determined about the centroidal axis of the cracked section and not the neutral axis.

Detailed discussions of the computation of I_{cr} may be found in Refs. 6 to 12. Jittawait⁸ developed formulas for the centroidal axis depth, y_{cr} , and the cracked moment of inertia, I_{cr} . They were developed using the commonly adopted assumptions of linear stress distribution and simple equilibrium relationships, in a way similar to the treatment of conventionally reinforced concrete columns, subject to combined axial force and bending.

Figs. 1 and 2 are approximations of the exact formulas. A program written for the Hewlett Packard microcomputer, and available from the Prestressed Concrete Institute,¹⁰ may be used to obtain more exact values of the cracked section properties as well as stresses before and after cracking.

The empirical equation:

$$I_{cr} = nA_{ps}d_{ps}^2(1 - \sqrt{\rho_p}) \quad (1)$$

given in the PCI Design Handbook is based on a report by the PCI Committee

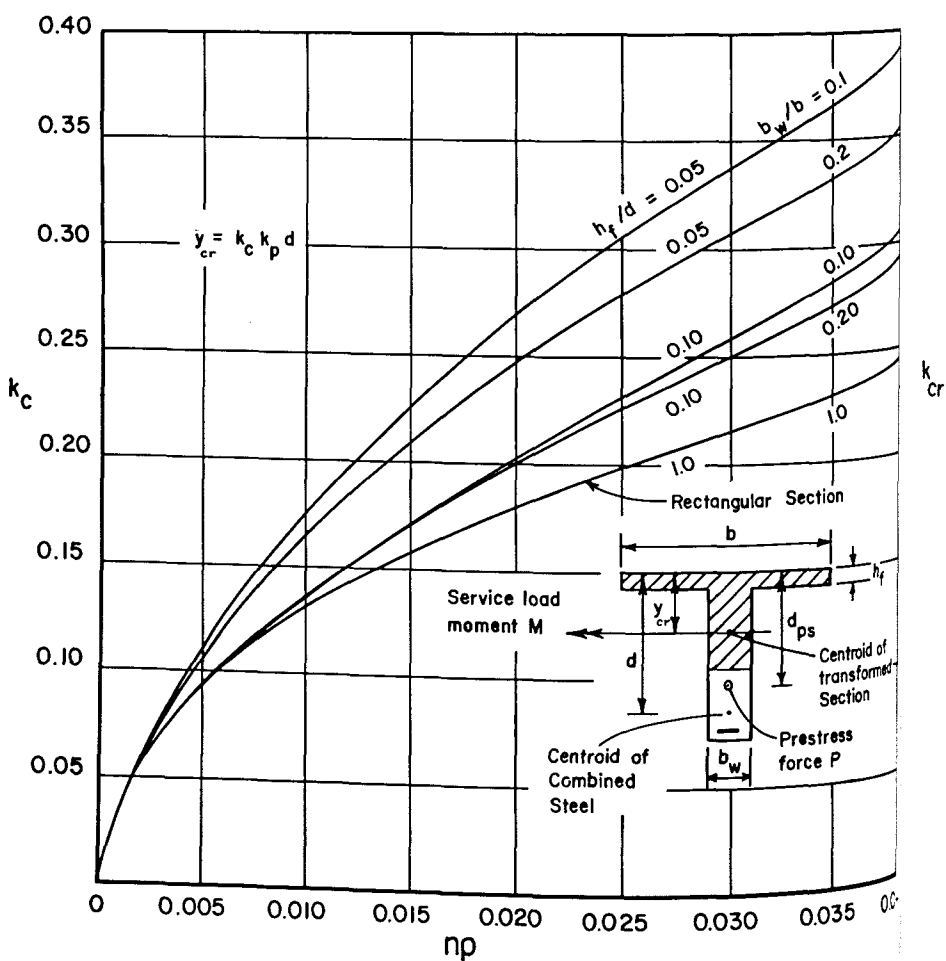
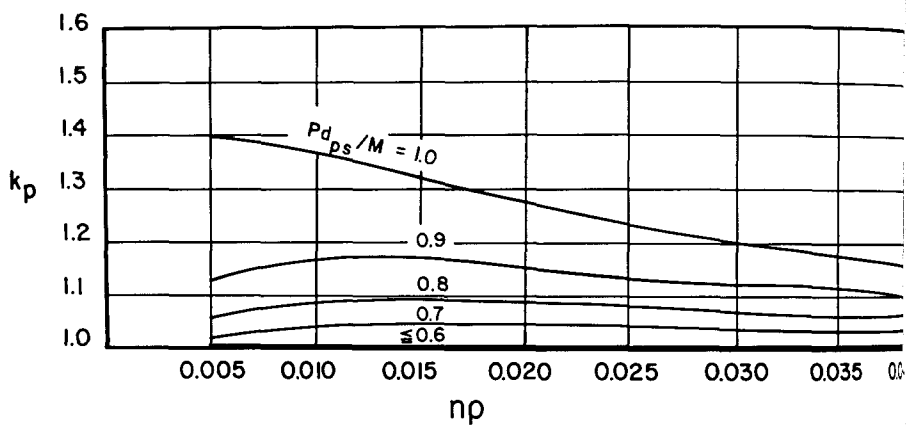


Fig. 1. Centroidal axis depth of cracked transformed section.

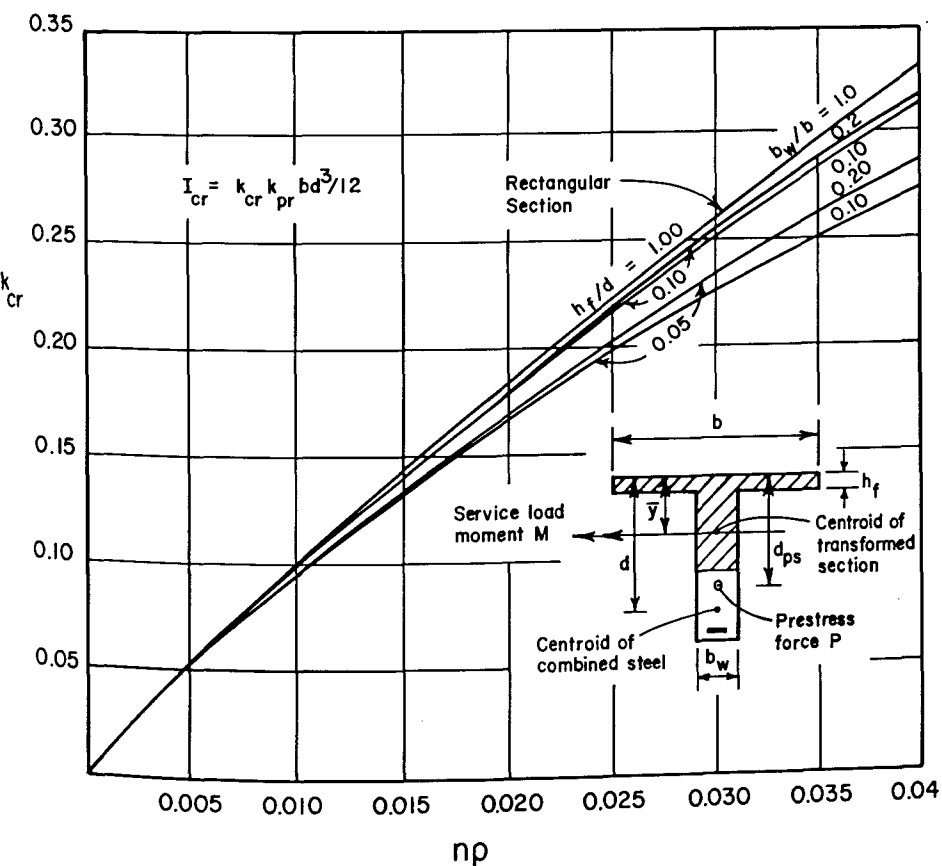
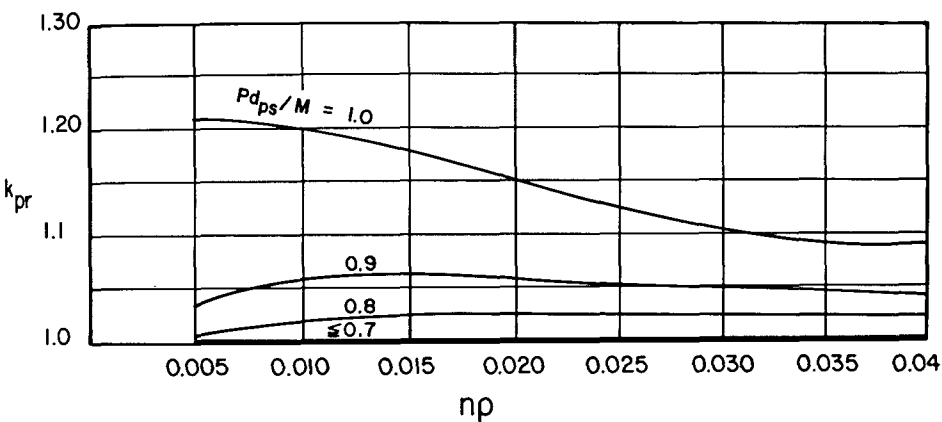


Fig. 2. Moment of inertia of cracked transformed section.

on Allowable Stresses.¹³ The formula is simple and appears to give reasonable results in the absence of nonprestressed steel, and when the effect of axial load is minor. Naaman⁹ has suggested the following modified version which accounts for the two types of steel in the section:

$$I_{cr} = \frac{(n_{ps}A_{ps}d_{ps}^2 + n_sA_sd_s^2)}{(1 - \sqrt{\rho_{ps} + \rho_s})} \quad (2)$$

The subscripts ps and s refer to prestressed and nonprestressed steel, respectively. The symbols n , A , and d are, respectively, modular ratio, steel area, and its effective depth. The parameter ρ is the ratio A/bd , where b is the width of the compression face of the member.

Moment-Curvature Relationship

The moment-curvature relationship for a conventionally reinforced cross section is illustrated in Fig. 3. The figure also shows the relationship for the same section if it were prestressed. Both relationships were prepared by the computer program given in Ref. 10 for the cross section given in Example 1. In order to understand the cross section behavior, it will be initially assumed that, upon cracking, concrete is incapable of resisting any tension. A moment, M_a , larger than the cracking moment, M_{cr} , produces curvature:

$$\phi_{cr} = (M_a - Pe_{cr})/E_c I_{cr} \quad (3)$$

where P is the prestress force, and e_{cr} is its eccentricity relative to the centroid of the cracked section. (Sign convention is given in Appendix B.) For the conventionally reinforced section, $P = 0$ and I_{cr} is constant. Therefore, the $M - \phi$ diagram is a straight line passing through the origin point. The drop in rigidity due to cracking is represented by the horizontal line at the M_{cr} level. For the prestressed section, both I_{cr} and y_{cr} (and in turn e_{cr}) are dependent on the loading level (see Figs. 1 and 2). Thus, the $M - \phi$ relationship is nonlinear.

It is important to note that the shift in the centroid of the cross section upon cracking, results in larger prestress force eccentricity, e_{cr} , than the uncracked member eccentricity. This is particularly significant in prestressed flanged members, such as the commonly used double tees which are characterized by relatively low steel area ratio, ρ . For these members, ignoring the increase in eccentricity upon cracking as implied in Refs. 14 and 15, could result in significant overestimation of deflection.¹⁶

Because concrete tensile strength is not zero, cracking does not extend to the neutral axis as assumed in standard cracked section analysis. In addition, uncracked concrete which exists between cracks in the tension zone, contributes to the stiffness of the member. These effects are often called "tension stiffening." If tension stiffening is accounted for, the $M - \phi$ diagram becomes continuous as indicated by the bold lines in Fig. 3. Empirical consideration of tension stiffening is discussed below.

Tension Stiffening

The following empirical equation is proposed here for the effective moment of inertia, I'_e to be used in calculating curvature:

$$I'_e = R^4 I_g + (1 - R^4) I_{cr} \quad (4)$$

with

$$R = f_r / f_{tm} \quad (5)$$

where f_r is the modulus of rupture of concrete and f_{tm} is the stress at the extreme tensile fiber assuming no cracking.

Eq. (4) performs an interpolation between I_g and I_{cr} . Note that, in practical applications, f_{tm} cannot reach infinity. Therefore, I'_e is always larger than I_{cr} where I_{cr} is the moment of inertia of the transformed section ignoring concrete in tension.

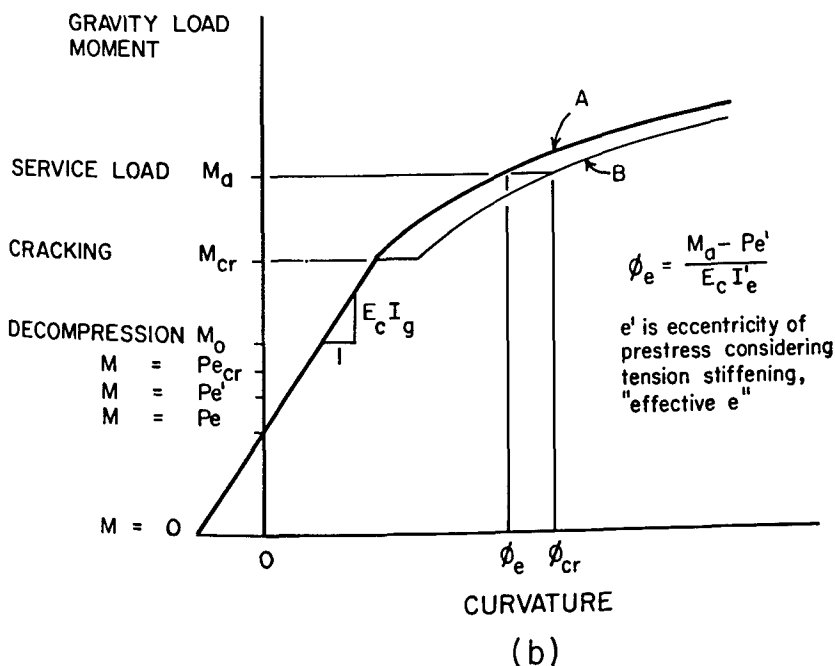
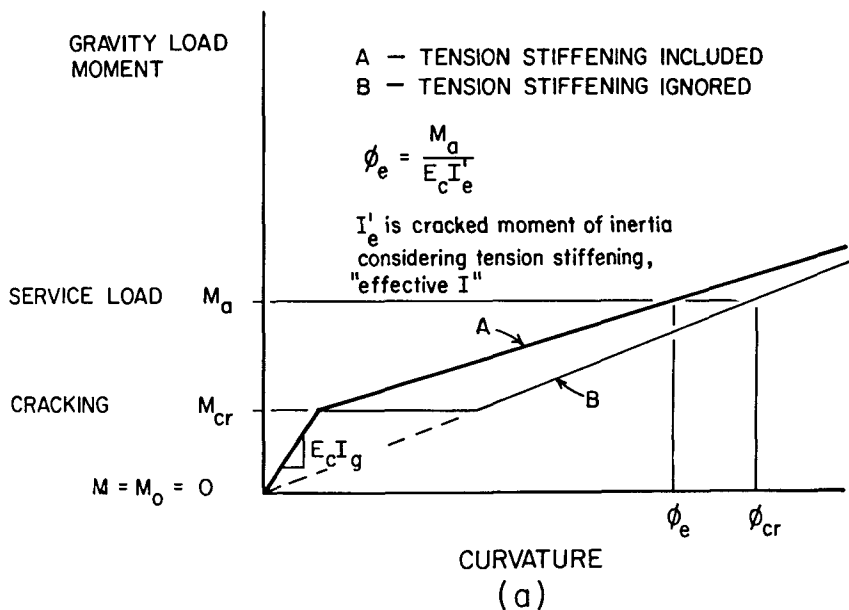


Fig. 3. Effect of tension stiffening in moment vs. curvature relationship:
(a) Conventionally reinforced section; (b) Prestressed section.

For prestressed concrete sections, it can be shown that:

$$(f_r/f_{tm}) = (M_{cr} - M_o)/(M_a - M_o) \quad (6)$$

where M_o is the decompression moment, defined as the moment which would cause the stress to become zero at the extreme precompressed fibers.¹⁰ Eq. (4) is an extension of the original I'_e equation developed by Branson¹⁷ for conventionally reinforced sections.

To determine the change in eccentricity after cracking, it is here suggested to employ the same interpolation ratio R to calculate an effective centroidal distance:

$$y_e = R^4 y_g + (1 - R^4) y_{cr} \quad (7)$$

where y_e , y_g , and y_{cr} are the effective, uncracked (with tension stiffening ignored) section centroidal distances to the extreme compression fibers (top surface in simple beams).

The values of I'_e and y_e for various sections along the member length are then used to calculate the curvatures at these sections. Eq. (3) may be used for this purpose with I'_e replacing I_{cr} and $(d_{ps} - y_e)$ replacing e_{cr} .

Another way to account for tension stiffening in reinforced concrete members is to interpolate between the curvatures ϕ_g and ϕ_{cr} of uncracked and cracked section instead of interpolation for section properties.^{18,19} The actual curvature:

$$\phi = R_1 \phi_g + (1 - R_1) \phi_{cr} \quad (8)$$

where R_1 is coefficient of interpolation:

$$R_1 = \beta_1 \beta_2 (f_{sr}/f_s)^2 \quad (9)$$

The symbols f_{sr} and f_s are stresses in the bottom steel in the cracked condition due to M_{cr} and M_a , respectively, combined with the prestress force; $\beta_1 = 1$ for high bond bars and $= 0.5$ for plain bars, respectively; $\beta_2 = 1$ for first loading and $= 0.5$ for loading applied in a sustained manner or for a large number of load cycles.

Trost²⁰ accounts for tension stiffening by interpolation between deflection values δ_g and δ_{cr} of uncracked and cracked structures:

$$\delta = R_2 \delta_g + (1 - R_2) \delta_{cr} \quad (10)$$

The interpolation coefficient:

$$R_2 = (M_n - M_a)^2 / (M_n - M_{cr})^2 \quad (11)$$

where M_n , M_a , and M_{cr} are moments, respectively, corresponding to the theoretical (nominal) strength, applied loads, and cracking load.

It is possible to analytically account for tension stiffening assuming an appropriate stress-strain relationship of concrete in tension. For example, the "strain softening" computer model by Bazant and Oh²¹ was reported to yield satisfactory results for conventionally reinforced beams. It should be possible to extend application of the same model to prestressed members.

Eqs. (8) and (10) appear to represent more direct approaches to tension stiffening consideration than do Eqs. (4) and (7). A study is needed to correlate the various interpolation methods with experimental results, especially on beams with practical dimensions and reinforcement content. The study should determine the method that offers the best compromise of accuracy and simplicity. Until then, consideration of this somewhat secondary effect, on prestressed concrete member deflection, may be done by any of the available methods.

Calculation of Deflection from Curvature

Numerical integration of the curvature may be used to obtain the deflection by any of the well known structural analysis methods, e.g., conjugate beam, moment area, or Newmark's integration technique.

Consideration should be given to the influence of tendon profile on curvature variation along the member, especially

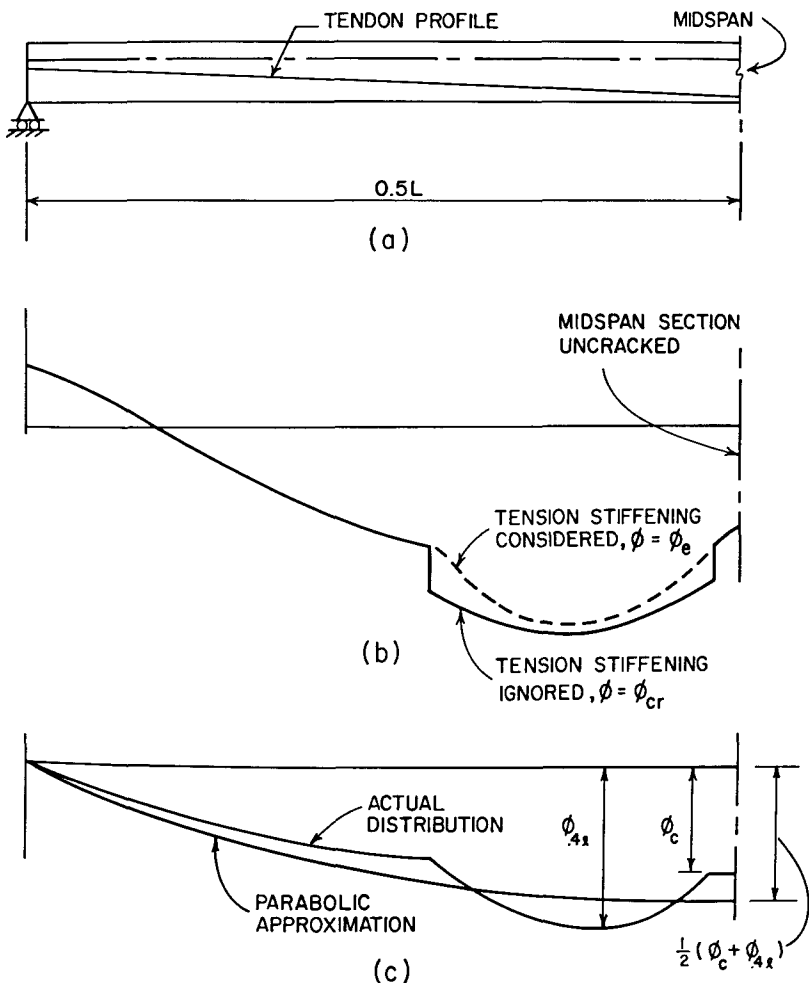


Fig. 4. Example of curvature distribution due to load combined with prestress in a cracked member with one-point depressed tendons: (a) Beam elevation; (b) Curvature due to total load plus prestress; (c) Live load curvature.

when one-point depressed tendons are used. Fig. 4 shows that, for this type of member, the most critical section is near $0.4l$ rather than midspan.

Two more observations could be made from Fig. 4. First, it is conservative to ignore tension stiffening for pre-

liminary deflection estimates. Secondly, the curvature of simply supported prestressed members can reverse sign in a similar manner to continuous rather than simply supported reinforced concrete members.

Methods of averaging I'_e for the entire

span of simply supported reinforced concrete beams, such as Eq. (9.7) of ACI 318-83, are not applicable to prestressed members, without due consideration of the curvature reversals and the relatively small cracked portion of the span.

It is recommended that curvatures be computed only at key sections along the span, and integrated to obtain deflection. As shown in Fig. 4c, and Example 1, a good estimate of the live load deflection of simply supported members with one-point depressed tendons can be found, in terms of the curvatures at the $0.4l$ and midspan sections by the following simple formula:

$$\delta = 5 [\phi_c + \phi_{0.4l}] l^2 / 96 \quad (12)$$

Eq. (12) is based on the assumptions that the live load curvature at member ends is zero, and that the curvature distribution is approximated as a parabola.

As mentioned before, cracking renders the problem nonlinear. Live load deflection cannot be obtained independently of consideration of dead load and prestress. First, curvatures due to total load plus prestress must be obtained, then those due to dead load plus prestress, using the geometric properties corresponding to each load level. The difference between the two quantities yields the live load curvatures to be used in Eq. (12).

TIME-DEPENDENT DEFLECTION

The time-dependent deflection is defined as the part of the deflection caused by creep and shrinkage of concrete and stress relaxation of the prestressing steel. Concrete creeps under prestress and sustained loads. This creep causes continual increase in camber or deflection. In the meantime, creep and shrinkage of concrete and stress relaxation of prestressing steel cause prestress loss which may be visualized as a negative increment of prestress.

The prestress loss, thus, contributes to the deflection of the member. In fact, it is an important contributor since the prestress in many applications "balances" a large portion of the dead load. It has been shown in a typical beam example, that computed deflection varies from 0.2 in. (downwards) to -1.6 in. (upwards) depending on the method of considering the prestress loss deflection.²²

The total long-term deflection is therefore equal to the algebraic sum of:

- (a) Creep deflection due to sustained load
- (b) Creep camber due to prestress, the prestress force being assumed constant and equal to its value at transfer
- (c) Prestress loss deflection

The deflections in Items (a) and (b) above are simply equal to the immediate value at load application multiplied by creep coefficient of concrete, which is defined as the ratio of creep strain to instantaneous strain due to a constant sustained stress. Its value is sensitive to such factors as the relative humidity and temperature of the surrounding air, the concrete age at loading, and the creep period since loading. It also depends on the concrete mix and curing method and on member size.

Long-term deflections can be determined using prediction methods such as those reported in Refs. 18 and 23. For average conditions and in the absence of more accurate information a value of the ultimate (in time) creep coefficient $C_u = 1.88$ is suggested in Refs. 4 and 23.

The creep coefficient is a function of concrete age at time of loading, and of loading duration. Introducing correction factors to C_u gives: creep coefficient $C_u' = 0.96$ for age at loading 1 to 3 days and load duration 40 to 60 days; $C_u' = 1.5$ for age at loading 40 to 60 days and infinite duration. Erection of the member and application of superimposed dead load is assumed to occur 40 to 60 days after release.

Table 2. Proposed time-dependent multipliers
(time-dependent δ = elastic $\delta \times$ multiplier).

Load condition	A Erection time		B Final time		C = B - A Long term	
	Formula	Average*	Formula	Average*	Formula	Average*
Initial prestress P_{co}	$1 + C_a$	1.96	$1 + C_u$	2.88	$C_u - C_a$	0.92
Prestress loss ΔP_c	$\alpha_a(1 + \chi C_a)$	1.00	$1 + \chi C_u$	2.32	$1 - \alpha_a + \chi(C_u - \alpha_a C_a)$	1.32
Member weight	$1 + C_a$	1.96	$1 + C_u$	2.88	$C_u - C_a$	0.92
Superimposed dead load†	0	0	$1 + C'_u$	2.50	$1 + C'_u$	2.50
Superimposed dead load‡	1.00	1.00	$1 + C'_u$	2.50	C'_u	1.50

* Assuming: $C_a = 0.96$, $C_u = 1.88$ and $C'_u = 1.50$, $\chi = 0.7$ and $\alpha_a = 0.6$ which approximately correspond to average conditions with relative humidity = 70 percent, concrete age at release = 1 to 3 days and erection at 40 to 60 days.

† Applied after nonstructural elements are attached to member.

‡ Applied before nonstructural elements are attached to member.

The presence of prestressed or non-prestressed reinforcement in a cross section restrains creep and shrinkage of concrete. However, creep deflection due to Causes (a) and (b) above are calculated as the product of C and the instantaneous deflection, using the properties of the concrete section without reinforcement. The restraining effect of the reinforcement is accounted for in Item (c). An alternative approach adopted in Ref. 19 is to use a reduction multiplier to the creep coefficient to account for the restraining effect of steel.

Martin²⁴ has proposed applying multipliers to the elastic deflections in order to obtain long-term deflections of precast members. This approach greatly simplifies the calculations, and is followed herein. Presented in Table 2 are the proposed formulas for the time-dependent multipliers.

Stress due to prestress loss is grad-

ually introduced, and thus should produce less creep compared to a stress introduced in its entirety at one instant and sustained thereafter. For this reason, the multiplier χC is used in Table 2 in lieu of C to calculate creep deflection associated with prestress loss; where χ is a value less than unity called the "aging coefficient" to be further discussed below.

PRESTRESS LOSS DEFLECTION

A valid prediction of deflection, due to loss of the compressive force in concrete, ΔP_c , is dependent on the accuracy of the magnitude of that prestress loss. There are several methods that can be used in arriving at a value for prestress loss. The reader may refer, for example, to reports by Zia et al.,²⁵ the PCI Com-

mittee on Prestress Loss,³ Tadros et al.,^{5,22} and the CEB-FIP Model Code.¹⁸ It should be noted that the deflection procedure presented herein is independent of the method chosen for estimating the prestress loss. However, if non-prestressed steel is present, it should not be ignored in calculating the prestress loss, ΔP_c .

A method of prestress loss calculation is presented in Appendix A. It is a simplified form of the procedure given in Refs. 5 and 22, which was found by Gurlitz²⁶ to be in close agreement with test results in comparison with several other prediction methods. One simplification of the method is replacement of the recovery parameter by the aging coefficient, χ .^{1,2}

Both parameters introduce the creep effects of the continually varying stresses caused by prestress loss. They employ numerical integration of assumed stress-time and creep-time functions. For the same time functions, both parameters should yield the same results. The aging coefficient, however, is simpler to use and is gaining wide acceptance in Europe.¹⁸

A second simplification adopted in Appendix A is replacement of the relaxation reduction factor chart⁵ by a simple formula. This has a somewhat secondary effect and use of an approximation for the reduction factor should have a minor effect on the prestress loss accuracy. The procedure in Appendix A is presented in steps similar in format to the simple steps given by Zia et al.²⁵ and by AASHTO.²⁷ Yet it is more general in that it includes the effects of the presence of nonprestressed steel and allows for flexibility in selecting material properties.

Once the magnitude of prestress loss ΔP_c is determined, the associated deflection may be calculated by an equation given in Table 1, which assumes parabolic variation of curvature due to ΔP_c . It is sufficient to determine ΔP_c at 0.4*l* for members with one-point depressed tendons or at midspan for other

cases and to consider that ΔP_c is constant over the member length.

The value of the aging coefficient ranges between 0.6 and 0.9. For 1 to 3 day load application, as is common for precast members, an approximate value of $\chi = 0.7$ may be used (see Ref. 28). For loading applications at a later concrete age χ is larger. However, for the sake of simplicity and since χ affects only the prestress loss deflection it is proposed that a value $\chi = 0.7$ be used.

To account for the difference in the magnitude of prestress loss at erection and final prestress loss the coefficient α_e is introduced in Table 2. It is the ratio of the time-dependent loss at erection to final prestress loss. It may be taken approximately equal to 0.6 for average environmental conditions, and for erection at 40 to 60 days after release.

The prestress loss force ΔP_c is assumed to act at the centroid of the prestressed and nonprestressed steel. Thus, the effect of the cross-sectional area of the nonprestressed steel and its location in the section on the deformation, are accounted for in the proposed method.

PCI DESIGN HANDBOOK METHOD

Table 3.4.1 of the PCI Design Handbook⁴ gives suggested multipliers as a guide to estimating long-term deflections for typical members. These multipliers were derived by extending the factor in Section 9.5.2.5 of ACI 318-77 to include the effect of prestress, the time-dependent loss of prestress, and the strength gain of the concrete after prestress release.²⁴

Examination of the method reveals that the environmental condition the member is subject to has been taken constant regardless of the geographic location, although it is known that members subject to a dry environment such as Arizona (USA) or Alberta (Canada) could exhibit a considerably larger

Table 3. Comparison of proposed average time-dependent multipliers and PCI Design Handbook multipliers.

Load conditions	Erection				Final			
	Proposed method		PCI method		Proposed method		PCI method	
	$\Delta P_c/P_{co} = 0.15$	$\Delta P_c/P_{co} = 0.35$	C_1 $A_s/A_{ps} = 0$	C_2^* $A_s/A_{ps} = 2$	$\Delta P_c/P_{co} = 0.15$	$\Delta P_c/P_{co} = 0.35$	C_1 $A_s/A_{ps} = 0$	C_2^* $A_s/A_{ps} = 2$
Initial prestress P_{co}	1.96	1.96	—	—	2.88	2.88	—	—
Prestress loss ΔP_c	1.00	1.00	—	—	2.32	2.32	—	—
Initial prestress less prestress loss	1.81 [†]	1.61 [†]	1.80	1.27	2.53 [‡]	2.07 [‡]	2.45	1.48
Member weight	1.96	1.96	1.85	1.28	2.88	2.88	2.70	1.57
Superimposed dead load	1.00	1.00	1.00	1.00	2.50	2.50	3.00	1.67

* $C_2 = \frac{C_1 + A_s/A_{ps}}{1 + A_s/A_{ps}}$ from PCI Design Handbook.

† Calculated from $\left(1.96 - 1.00 \frac{\Delta P_c}{P_{co}} \right)$.

‡ Calculated from $\left(2.88 - 2.32 \frac{\Delta P_c}{P_{co}} \right)$.

creep than those built in a more humid environment such as Florida (USA).

A comparison of the PCI Design Handbook multipliers and those in Table 2 shows that the multipliers are comparable if environmental conditions are average and if nonprestressed steel is not present (see for example Table 3). One exception is the multiplier for the superimposed dead load deflection at final time (2.50 versus 3.00). It would seem reasonable to have a relatively small multiplier for the case of superimposed dead load which is applied later than the load due to member weight.

The PCI Design Handbook provides a reduction factor, to be applied to the time-dependent multipliers in order to account for the presence of nonprestressed steel, as shown in Table 3. The reduction factor is a function of A_s/A_{ps} ,

and is applied in the Handbook to both camber due to prestress and deflection due to gravity loads. It is based on a study by Shaikh and Branson²⁹ of members that exhibited camber under prestress combined with dead load. The factor was later adopted by ACI Committee 435³⁰ for camber reduction only.

The accuracy of the correction factor, as given in the Handbook, is questionable for two reasons. First, the location of the nonprestressed steel is as important as its area in determining its influence. Bottom nonprestressed steel restrains creep and shrinkage of the surrounding concrete, relative to the top fibers and, therefore, contributes an *increase* in net time-dependent downward deflection (or reduction in net camber). Secondly, the reduction factor does not relate the steel area to the concrete area

Table 4. Test beam details.

Beam No.	Beam type	Tension zone	Prestressed steel		Nonprestressed steel		Total area, in. ²	Prestress force at release, kips	Super-imposed dead load, lb/ft
			Amount, in.	Area, in. ²	Amount, in.	Area, in. ²			
B-1	Fully pre-stressed	Un-cracked	1 - $\phi \frac{7}{16}$	0.108	—	—	0.108	19	100
B-2	Partially pre-stressed	Un-cracked	2 - $\phi \frac{3}{8}$	0.160	1 - $\phi \frac{3}{8}$	0.080	0.240	12.5	100
B-3	Partially pre-stressed	Cracked	1 - $\phi \frac{3}{8}$	0.080	2 - $\phi \frac{3}{8}$	0.160	0.240	6.3	150
B-4	Reinforced	Cracked	—	—	1 - $\phi \frac{7}{16}$	0.100	0.108	0	50

Notes:

1. All beams are simply supported, span = 14 ft, and cross section = 6 x 8 in.
2. All tendons are seven-wire stress-relieved strands, $f_{pu} = 250$ ksi.
3. Specified ultimate strength of concrete at age 28 days, $(f'_c)_{28d} = 5000$ psi.

restrained by its presence.

It is interesting to note that this latter point is applicable to the effect of compression reinforcement A'_c in conventionally reinforced members. For these members, the deflection reduction factor which was originally given in terms of (A'_c/A_s) , where A_s is the tension steel area, has recently been changed to a more rational factor, in terms of (A'_c/bd) . See the ACI 318-83 Code, Section 9.5.2.5.

The need for an empirical reduction factor is eliminated in the proposed procedure by rationally accounting for the presence of nonprestressed steel in the magnitude and location of the prestress loss ΔP_c . Table 3 gives a comparison of both the proposed procedure and the PCI Design Handbook multipliers for two cases.

The first case is when $A_s = 0$, and $\Delta P_c/P_{co}$ is assumed = 0.15 as implied in the Handbook multipliers. Addition of nonprestressed steel of area $A_s = 2A_{ps}$ at the same level as the prestressed steel

roughly increases the prestress loss to $\Delta P_c = 0.35 P_{co}$.

It may be noted in the comparison, that in the one case where the Handbook reduced multiplier is appropriate (because it reduces camber), the correction appeared excessive (2.45 versus 1.48). This confirms Gurlitz' finding²⁸ that, for test beams with A_s/A_{ps} values in excess of 2, the correction was excessive.

As indicated earlier, provision of nonprestressed mild steel generally increases the overall flexural stiffness of the member since a relatively large mild steel area would be needed to substitute for stronger prestressing strands. The elastic deflections are thus reduced, corresponding to an increase in the transformed moment of inertia.

This effect is often neglected if the member is uncracked since I_g is usually used in lieu of the uncracked transformed section moment of inertia. However, the effect of nonprestressed steel on I_{cr} is much more pronounced, as in

licated by Eqs. (1) and (2), and should be taken into account. This is discussed further in Example 2.

SUPPORTING TEST DATA

Testing was conducted⁸ to study deflection behavior of four simply supported beams of equal rectangular cross section, span length, and steel eccentricity. The beams ranged from fully prestressed to conventionally reinforced (see Table 4). Deflection was measured under dead load, sustained for a period of 180 days, as well as instantaneous load.

Measurements were also taken of creep, shrinkage, and strength development with time. Comparison between test results and values predicted by the proposed method indicate a close agreement as represented by Fig. 5. Details of the experiment may be found in Ref. 8.

PROPOSED CALCULATION STEPS

The following is a summary of the steps to be followed to determine deflections in accordance with the proposed method. To simplify the organization of data, it is suggested that values be arranged in a chart form, such as that shown in Table 5.

1. Estimate the prestress loss using the procedure outlined in Appendix A.

2. Determine instantaneous deflections due to initial prestressing force, prestress loss, member weight, and superimposed dead load, using properties of uncracked concrete section without reinforcement. Table 1 or another design aid may be used.

3. Using multipliers from Table 2, determine time-dependent effects on deflection in Step 2. This will result in elastic-plus-creep deflections at "Erection Time," and at time infinity "Final Time," as well as the difference be-

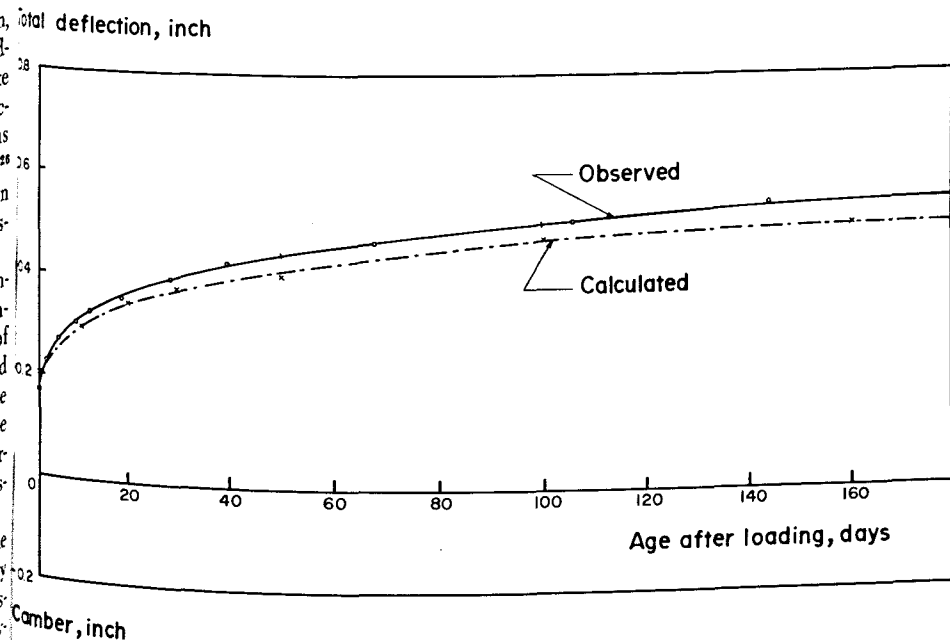


Fig. 5. Total time-dependent deflection of Test Beam B-3.

Table 5. Deflection chart (Example 1).

Load condition	A	B	C		D		E = D - C	
	Elastic	Release	At erection		Final "ultimate"		Long-term	
	δ	δ	Multi-plier	δ	Multi-plier	δ	Multi-plier	δ
Initial prestress	-3.23	-3.23	1.96	-6.33	2.88	-9.30	0.92	-2.97
Prestress loss	0.84	—	1.00	0.84	2.32	1.95	1.32	1.11
Member weight	3.00	3.00	1.96	5.88	2.88	8.64	0.92	2.76
Superimposed dead load*	0.48	—	—	—	2.50	1.20	2.50	1.20
Live load	2.73	—	—	—	—	2.73	—	2.73
Total	—	-0.23	—	0.39	—	—	—	4.83

*For this example, the superimposed dead load is assumed to be fully applied after nonstructural elements are attached to member.

Note: Deflection is in inches. 1 in. = 25.4 mm.

tween deflections at these two times which is labeled "Long Term." See Table 5 for illustration.

4. If the member cracks under full service loads, determine the cracked section properties from Figs. 1 and 2 and the cracked member live load deflection. If the total deflection, computed thus far, satisfies the design limitations, i.e., ACI 318-83, Table 9.5b, the designer may elect to terminate the calculations. Otherwise, a refined value for the live load deflection may be obtained from Step 5.

5. If the member is cracked, concrete tension stiffening effects may be empirically taken into account using interpolation Eqs. (4) and (7), or another means.

One-point depressed pretensioning tendons are used as shown in Fig. 4. Assume span = 70 ft. Other data are:

Concrete Properties

$f_{ci}' = 3,500$ psi
 $f_c' = 5,000$ psi
 $f_r = 530$ psi
 $E_{ci} = 3,587$ ksi
 $E_c = 4,287$ ksi
Creep coefficients:
 $C_u = 1.88, C_u' = 1.50$
Free shrinkage, $\epsilon_{shu} = 560 \times 10^{-6}$

Prestressing Steel

Ten 1/2-in. diameter, 270 ksi stress relieved strands
 $e_c = 13.40$ in., $e_e = 3.79$ in.
 $f_{pst} = 189$ ksi
 $A_{ps} = 1.53$ in.², $E_{ps} = 28,000$ ksi
Intrinsic relaxation, $L_r = -16.1$ ksi

Nonprestressed Steel

Two #8 bars, $e = 15.15$ in.
 $A_s = 1.58$ in.², $E_s = 28,000$ ksi

Section Properties

$A_g = 401$ in.², $I_g = 20,985$ in.⁴
 $y_b = 17.15$ in., $y_t = 6.85$ in.

NUMERICAL EXAMPLES

EXAMPLE 1

Calculate the central deflection of a partially prestressed simply supported beam shown in cross section in Fig. 6.

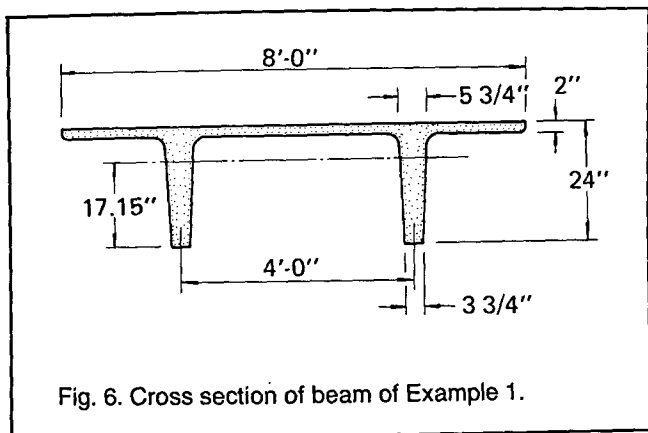


Fig. 6. Cross section of beam of Example 1.

Gravity Loads

Member dead weight = 418 plf
 Superimposed dead load = 80 plf
 Live load = 200 plf

Solution

Moments at midspan: $M_d = 3,072$ in.-kips, $M_{sd} = 588$ in.-kips, and $M_l = 1,470$ in.-kips. Moments at 0.4l: $M_d = 2,949$ in.-kips, $M_{sd} = 564$ in.-kips, and $M_l = 1,411$ in.-kips.

Step 1 — Ultimate Prestress Loss, ΔP_c , at a Section 0.4l From Support

Eccentricity of A_{ps} at 0.4l:

$$e_{ps} = (0.8)(13.40) + (0.2)(3.79) = 11.48 \text{ in.}$$

This corresponds to a total steel area eccentricity:

$$e_{ts} = \frac{(11.48)(1.53) + (15.15)(1.58)}{1.53 + 1.58} = 13.34 \text{ in.}$$

With an initial estimate of $P_{co} = 0.9 P_i = 260.3$ kips, Eq. (A2) yields:

$$f_{cr} = \frac{260.3}{401} + \frac{(260.3)(11.48)(13.34)}{20,985} - \frac{(2,949)(13.34)}{20,985} = 0.674 \text{ ksi}$$

Eq. (A1) yields the corresponding

elastic shortening loss, using:

$$n_i = 28,000/3,587 = 7.81, \\ ES = (7.81)(0.674) = 5.3 \text{ ksi}$$

Thus,

$$f_{ps0} = f_{psi} - ES = 189 - 5.3 = 183.7 \text{ ksi} \\ \text{and } f_{ns0} = -5.3 \text{ ksi.}$$

An improved value of P_{co} may be found from Eq. (A3):

$$P_{co} = (183.7)(1.53) + (-5.3)(1.58) = 272.7 \text{ kips}$$

A second iteration gives:

$$f_{cr} = 0.795 \text{ ksi and } P_{co} = 269.9 \text{ kips.}$$

These two values are used in further calculations.

By substitution into Eq. (A5) with:

$$n_i A_{ts}/A_g = (7.81)(3.11)/401 = 0.0606, \\ (1 + e^2/r^2) =$$

$$1 + (13.34)^2(401)/20,985 = 4.40,$$

and $(1 + \chi C_u) = 1 + (0.7)(1.88) = 2.32$, the coefficient:

$$K = [1 + (0.0606)(4.40)(2.32)]^{-1} = 0.618$$

Eq. (A4) gives the shrinkage loss:

$$SH = (0.618)(560 \times 10^{-6})(28,000) = 9.69 \text{ ksi}$$

The creep loss [Eq. (A6)], with:

$$f_{cds} = (-564)(13.34)/20,985 = -0.359 \text{ ksi}$$

gives a value of:

$$CR = (0.618)[(7.81)(1.88)(0.795) + (6.53)(1 + 1.5)(-0.359)] = 3.59 \text{ ksi}$$

Eq. (A8) yields a relaxation reduction factor:

$$\psi = 1 - \frac{3(9.69 + 3.59)}{183.7}$$

$$= 0.783$$

Thus, the relaxation loss, using Eq. (A7):

$$REL = -(0.783)(0.618)(-16.1)$$

$$= 7.79 \text{ ksi}$$

The total time-dependent loss of compression in concrete, using Eq. (A9):

$$\Delta P_c = -(3.11)(9.69 + 3.59)$$

$$- (1.53)(7.79)$$

$$= -53.2 \text{ kips}$$

Step 2 — Immediate Deflection

According to Table 1, the curvature due the initial prestress, P_{co} , at midspan:

$$\phi_c = - \frac{(269.9)(13.4)}{(3,587)(20,985)}$$

$$= -4.81 \times 10^{-5} \text{ in.}^{-1}$$

Similarly, the end section curvature:

$$\phi_e = -1.36 \times 10^{-5} \text{ in.}^{-1}$$

and the midspan deflection:

$$\delta = \left[(-4.81) \frac{(840)^2}{8} \right]$$

$$- \left[(-4.81 + 1.36) \frac{(840)^2}{24} \right] 10^{-5}$$

$$= -3.23 \text{ in.}$$

The immediate self weight deflection (using E_{ci}) can be found in a similar way to be = 3.00 in. The superimposed dead load deflection (using E_c) is 0.48 in.

Step 3 — Time-Dependent Deflections

The force ΔP_c develops gradually between prestress release and time infinity. The change in curvature at any section during this period is:

$$(\Delta P_c e_{it}/E_{ci} I_g)(1 + \chi C_u).$$

The first term, $\Delta P_c e_{it}/E_{ci} I_g$, represents the curvature which would instantaneously occur if the entire value of ΔP_c were applied at prestress release. The values of this hypothetical "elastic" curvature at midspan and at the ends are: 1.01×10^{-5} and $0.68 \times 10^{-5} \text{ in.}^{-1}$

These values reflect the assumption

that ΔP_c is located at the centroid of the combined steel area. The corresponding midspan and end eccentricities are 14.29 and 9.56 in. The "elastic" deflection, due to ΔP_c , according to Table 1 is 0.84 in.

The multiplier $(1 + \chi C_u) = 2.32$ is then applied to the elastic value to give ultimate deflection due to prestress loss = 1.95 in. Assuming $\alpha_a = 0.6$ and $C_a = 0.96$, the deflection at erection time (see multipliers in Table 2) is:

$$0.6(1 + 0.96)0.84 = 0.99 \text{ in.}$$

The time-dependent deflections due to initial prestress, dead load, and superimposed dead load are obtained by applying the appropriate multipliers according to Table 2, to the above calculated immediate deflections. The results are shown in Table 5.

Step 4 — Immediate Live Load Deflection

The bottom fiber concrete stress at the 0.4l section using uncracked section analysis, due to full load moment of: $2,949 + 564 + 1,411 = 4,924 \text{ in.-kips}$ and effective prestress: $P_{ce} = 269.9 - 53.2 = 216.7 \text{ kips}$ can be calculated:

$$f_{tm} = \frac{216.7}{401} + \frac{216.7(11.48)(17.15)}{20,985}$$

$$- \frac{4,924(17.15)}{20,985} = -1.451 \text{ ksi}$$

This tensile stress is in excess of the modulus of rupture, indicating cracking of the member. The cracked section properties may be found from the charts in Figs. 1 and 2, given the following parameters:

$$Pd_p/M = (216.7)(18.33)/4,924 = 0.81$$

$$n\rho = (6.53)(3.11)/(96)(20.2) = 0.010$$

$$b_w/b = 9.5/96 = 0.1, \text{ and}$$

$$h_f/d = 2/20.2 = 0.1.$$

Note here that the decompression force is taken approximately equal to the effective prestress force, and that the depth d is to the centroid of the total steel area.

Fig. 1 yields:

$y_{cr} =$
 $I_{cr} =$
 $=$
The
prestressed
 $\phi =$
The
curvature
by dead
cracked
 ϕ_{live} loc
Simi
midspan
(12), an
tion ca
 $\delta =$
 $=$
Step 5
Stiffen
Impr
empiri
sion st
cussed
this ex
to calc
ment o
At 0.
 $R =$
 $I_e =$
 $=$
 $y_e =$
The
ture [E
live lo
in. $^{-1} =$
Simi
vature
spondi
Furth
will re
tures at
PCI JOURNAL

$$y_{cr} = (0.143)(1.1)(20.2) = 3.18 \text{ in.}, \text{ and} \\ I_{cr} = (0.11)(1.02)(96)(20.2)^3/12 \\ = 7,400 \text{ in.}^4$$

The curvature due to full load plus prestress, at $0.4l$, using Eq. (3):

$$\phi = \frac{4,924 - (216.7)(18.33 - 3.18)}{(4,287)(7,400)} \\ = 5.17 \times 10^{-5} \text{ in.}^{-1}$$

The live load curvature is equal to this curvature less the curvature produced by dead load plus prestress (using uncracked section properties).

$$\phi_{\text{live load}} = 5.17 \times 10^{-5} \\ - \frac{3,513 - 216.7(11.48)}{(4,287)(20,985)} \\ = 4.03 \times 10^{-5} \text{ in.}^{-1}$$

Similarly, the live load curvature at midspan $= 3.45 \times 10^{-5} \text{ in.}^{-1}$. Using Eq. (12), an estimate of the live load deflection can be made:

$$\delta = 5[3.45 + 4.03](10)^{-5} \frac{(840)^2}{96} \\ = 2.75 \text{ in.}$$

Step 5 — Consideration of Tension Stiffening

Improved results may be obtained by empirical consideration of concrete tension stiffening. One of the methods discussed in this paper may be used. For this example, Eqs. (4) and (7) are used to calculate adjusted "effective" moment of inertia and centroidal depth.

At $0.4l$:

$$R = (0.530/1.451)^4 = 0.02, \\ I_e = 0.02(20,985) + 0.98(7,400) \\ = 7,670 \text{ in.}^4, \text{ and} \\ y_e = 0.02(6.85) + 0.98(3.18) = 3.25$$

The corresponding total load curvature [Eq. (3)] is $5.04 \times 10^{-5} \text{ in.}^{-1}$ and the live load curvature is $(5.04 - 1.14)10^{-5} \text{ in.}^{-1} = 3.9 \times 10^{-5} \text{ in.}^{-1}$.

Similarly, the midspan live load curvature is $3.32 \times 10^{-5} \text{ in.}^{-1}$ and the corresponding live load deflection $= 2.65 \text{ in.}$

Further improvement of the accuracy will result from computing the curvatures at short intervals, and then numer-

ically integrating these curvatures over the span length. This refinement results in a live load $\delta = 2.73 \text{ in.}$ A summary of the deflections of the beam is given in Table 5.

The calculated live load deflections is about $l/300$. This is slightly larger than the limit of $(l/360)$ set by the ACI 318-83 Code for floors not supporting or attached to nonstructural elements likely to be damaged by large deflections. The member would be satisfactory in similar roof construction (with $\delta_{max} = l/180$) but not in construction requiring attachment of nonstructural elements, due to the excessive long-term deflection ($4.83 \text{ in.} > l/240 = 3.50 \text{ in.}$).

EXAMPLE 2

In this example, comparison is made between three beams in order to illustrate the influence of prestressing level and of presence of nonprestressed steel. Table 6 gives the difference in prestress force and reinforcement in the three beams. Note that Beam A is identical to that analyzed in the PCI Design Handbook, Examples 3.2.8, and 3.4.1, except that the live load is reduced from 35 to 25 psf. Beam C is the beam of Example 1 in this paper. The deflections are calculated by both the proposed method and the PCI Design Handbook method.

The results indicate that the total initial and time-dependent deflections are sensitive to the magnitude of the prestress force. A slight change in the deflection due to prestress results in a much more pronounced total (net) deflection because of the opposite effects of prestress and gravity loads. The flat rate of prestress loss (10 percent elastic loss, and 15 percent time-dependent loss) results in about $\frac{1}{4} \text{ in.}$ error in the initial deflection (camber) and a larger error in the final deflection, in Beam B. Errors in Beam A deflections are not as large.

Substitution of four $\frac{1}{2} \text{ in.}$ strands ($A = 0.612 \text{ in.}^2$) with two #8 bars ($A = 1.58$

Table 6. Influence of prestress level and reinforcement on deflection.

Input data:		Beam A*		Beam B		Beam C	
Prestress force just before release P_i		405.0		289.2		289.2	
Reinforcement		14 strands		14 strands		10 strands plus 2 #8 bars	
For other data, see Example 1							
		Pro- posed method	PCI Design Hand- book	Pro- posed method	PCI Design Hand- book	Pro- posed method	PCI Design Hand- book
Results:							
Prestress force just after release, P_{co}		375.3	364.0	274.6	260.3	269.9	260.3
Deflection at release due to:							
Prestress		-4.64	-4.49	-3.39	-3.15	-3.23	-3.15
Self weight		<u>3.00</u>	<u>3.00</u>	<u>3.00</u>	<u>3.00</u>	<u>3.00</u>	<u>3.00</u>
Total deflection at release		-1.64	-1.41	-0.39	-0.15	-0.23	-0.15
Time-dependent prestress loss, ΔP_c		-71.7	-54.6	-36.8	-39.0	-53.2	-39.0
Final "ultimate" time-dependent deflection due to:							
Prestress		-11.00	-11.00	-8.55	-7.72	-7.35	-5.39
Self weight		8.64	8.10	8.64	8.10	8.64	5.52
Superimposed dead load		<u>1.20</u>	<u>1.44</u>	<u>1.20</u>	<u>1.44</u>	<u>1.20</u>	<u>0.96</u>
Total time-dependent deflection		-1.16	-1.46	1.29	1.82	2.49	1.13
Geometric properties under full load:							
0.4l	Moment of inertia	20985	20985	4180	—	7400	—
	Prestress force eccentricity	11.78	11.78	16.06	—	15.15	—
Mid-span	Moment of inertia	20985	20985	5160	5541	7850	3890
	Prestress force eccentricity	13.65	13.65	17.62	13.65	17.01	13.65
Live load curvature x 10 ⁶ :							
End section		0	0	0	0	0	0
0.4l section		15.7	15.7	53.8	47.2	40.3	65.3
Midspan section		16.4	16.4	37.9	49.1	34.5	68.0
Live load deflection		1.21	1.21	2.76	3.61	2.73	5.00

*End section eccentricity used is $e = 4.29$ in., which is consistent with the PCI Design Handbook Example 3.2.8, but slightly different from $e = 3.79$ in. in Example 3.4.1.

Note: Forces are given in kips, and dimensions in inches. 1 kip = 4.45 kN; 1 in. = 25.4 mm.

in.²) provides additional restraint to concrete deformation in the bottom of the beam. This results in higher initial and time-dependent prestress losses in Beam C than in Beam B, and a correspondingly larger downward deflection (2.49 in. versus 1.29 in.). The PCI Design Handbook empirical multipliers lead to

reduction of the time-dependent deflection from 1.82 to 1.13 in., rather than an increase from 1.29 to 2.49 in. in the proposed method.

One may pose the following question since Beam C contains more steel than Beam B, how could Beam C, which is stiffer, have more loss of prestress and

long-term
answer
dependent
loss, Δ
as the
crete,
the p
between
the co
nonpr
the qu
puting
format
Exa
Beam
Beam
the p
This i
influe
dent
-7.35
flectio
net re
net de
tion.
The
much
cracki
Crack
less th
I. How
less th
partly
the in
tricity
agree
exists
and w
tain r
Howe
Beam
Not
Handb
the pr
the ar
sidera
stresse
than F
crease
load d
It is

long-term deflection than Beam B? The answer to this question becomes evident if one remembers that the prestress loss, ΔP_c , is defined in the present work as the loss of compression force in concrete, rather than the loss of tension in the prestressed steel. The difference between the two quantities is equal to the compression force developed in the nonprestressed steel. The force ΔP_c is the quantity that must be used in computing the concrete stresses and deformation.

Examination of Table 6 shows that Beam C has a larger prestress loss than Beam B, due to the restraint caused by the presence of nonprestressed steel. This increase in ΔP_c has a significant influence in reducing the time-dependent prestress camber (-8.55 versus -7.35 in.). Since the gravity load deflections are the same in both beams, the net result is a significant increase in the net downward time-dependent deflection.

The live load deflection of Beam B is much larger than that of Beam A due to cracking as a result of reduced prestress. Cracking drops the moment of inertia to less than one-quarter of the gross section I . However, the deflection of Beam B is less than four times that of Beam A, partly due to the moderating effect of the increase in prestress force eccentricity upon cracking. Reasonably close agreement between the two methods exists for the uncracked beam, Beam A, and when a cracked beam does not contain nonprestressed steel, Beam B. However, a great difference exists for Beam C, 2.73 versus 5.00 in.

Note that the current PCI Design Handbook equation for I_{cr} , [Eq. (1) of the present paper] does not account for the area of nonprestressed steel. Consideration of the presence of nonprestressed steel, by using Eq. (2) rather than Eq. (1), results in a significant increase in I_{cr} and a drop in Beam C live load deflection (from 5.00 to 2.46 in.).

It is interesting to note that the live

load deflections, by the proposed method, of Beams B and C are about equal although Beam C contains more steel and would be expected to deflect less under live load. However, due to the fact that the prestress loss ΔP_c is greater, and therefore the effective prestress is smaller, the beam begins to crack under a lower load than Beam B. The live load thus causes cracking to develop in Beam C over a greater portion of the span length than in Beam B. The increase in the amount of cracking appears to offset the increase in the cracked member stiffness resulting from the presence of nonprestressed steel.

CONCLUSIONS

1. The method proposed here contains simple steps in which the time-dependent effects, the presence of nonprestressed steel, and the effects of cracking are rationally accounted for. Design charts are included which can be used to determine cracked section moment of inertia and centroidal depth.

2. The multipliers for time-dependent effects given here can be used for various environmental conditions, by selecting representative creep coefficients and free shrinkage value.

3. It is shown that deflection due to prestress losses must be correctly considered in order to obtain reliable deflection estimates, especially when the dead load and the load "balanced" by prestress are nearly equal.

4. The presence of nonprestressed mild bar reinforcement causes a significant restraint to the surrounding concrete and substantially affects the long-term deflections. This corresponds to an increase in the loss, ΔP_c , in the compressive force in concrete. The proposed method for calculating ΔP_c and its eccentricity, or another method that rationally accounts for the effects of nonprestressed steel, should be used in accurate deflection calculations.

5. The geometric properties of

cracked sections are influenced by the presence of axial force combined with bending moment, particularly for flanged members where the steel area ratio is relatively low. Also replacement of high strength tendons with a larger amount of nonprestressed mild reinforcing bars can considerably increase the cracked section rigidity.

6. The stiffening effects caused by consideration of uncracked tensioned concrete in deflection analysis requires the determination of two quantities, the effective moment of inertia, and the effective eccentricity of prestress force. These two parameters must, by definition, lie between the uncracked section properties, and those of prestressed

cracked sections, with concrete in tension ignored.

7. Test data show a close correlation between observed deflections and those calculated by the proposed method.

8. When the proposed method is compared to the PCI Design Handbook method, it is seen that there is a close agreement in the deflection multipliers for average environmental conditions and when nonprestressed steel is absent.

ACKNOWLEDGMENT

Initial stages of the research reported in this paper were sponsored by a PCI Research Fellowship Grant.

* * *

REFERENCES

1. Trost, H., "Auswirkungen des Superpositionsprinzips auf Kriech- und Relaxationsprobleme bei Beton und Spannbeton," *Beton und Stahlbetonbau*, V. 62, No. 10, 1967, pp. 230-238; No. 11, 1967, pp. 261-269.
2. Bazant, Z. P., "Prediction of Concrete Creep Effects Using Age-Adjusted Effective Modulus Method," *ACI Journal*, V. 69, No. 4, April 1972, pp. 212-217.
3. PCI Committee on Prestress Losses, "Recommendations for Estimating Prestress Losses," *PCI JOURNAL*, V. 20, No. 4, July-August 1975, pp. 108-126. See Reader Comments, *PCI JOURNAL*, V. 21, No. 2, March-April 1976, pp. 108-126.
4. *PCI Design Handbook Precast Prestressed Concrete*, Second Edition, Prestressed Concrete Institute, Chicago, Illinois, 1978.*
5. Tadros, M. K., Ghali, A., and Dilger, W. H., "Effect of Nonprestressed Steel on Prestress Loss and Deflection," *PCI JOURNAL*, V. 22, No. 2, March-April 1977, pp. 50-63.
6. Moustafa, S. E., "Design of Partially Prestressed Concrete Flexural Members," *PCI JOURNAL*, V. 22, No. 3, May-June 1977, pp. 12-19. See Reader Comments, *PCI JOURNAL*, V. 23, No. 3, May-June 1978, pp. 92-105.
7. Naaman, A. E., and Siriakson, A., "Serviceability Based Design of Partially Prestressed Beams," *PCI JOURNAL*, V. 24, No. 2, March-April 1978, pp. 64-89.
8. Jittawit, V., "Deflection of Partially Prestressed Concrete Members," MSCE thesis directed by M. K. Tadros, Department of Civil Engineering, West Virginia University, 1979.
9. Naaman, A. E., *Prestressed Concrete Analysis and Design - Fundamentals*, First Edition, McGraw Hill Book Co., New York, N.Y., 1982, 670 pp.
10. Tadros, M. K., "Expedient Service Load Analysis of Cracked Prestressed Concrete Beams," *PCI JOURNAL*, V. 27, No. 6, Nov.-Dec. 1982, pp. 86-111. See also Reader Comments, *PCI JOURNAL*, V. 28, No. 6, Nov.-Dec. 1983, pp. 137-158.
11. Nilson, A. H., "Flexural Stresses After Cracking in Partially Prestressed Beams," *PCI JOURNAL*, V. 21, No. 4, July-August 1976, pp. 72-81.
12. Inomata, S., "A Design Procedure for Partially Prestressed Concrete Beams Based on Strength and Serviceability," *PCI JOURNAL*, V. 27, No. 5, Sept.-Oct. 1982, pp. 100-116. See also Reader Comments, *PCI JOURNAL*, V. 28, No. 4, July-August 1983, pp. 162-166.
13. PCI Committee on Allowable Stresses in Prestressed Concrete Design, "Allowable Tensile Stresses for Prestressed Concrete," *PCI JOURNAL*, V. 15, No. 4, Feb. 1970, pp. 37-42.
14. Branson, Dan E., and Trost, H., "Unified Procedures for Predicting the Deflection and Centroidal Axis Location of Partially Cracked Nonprestressed and Prestressed Concrete Members," *ACI Journal*, Proceedings V. 79, No. 2, March-April 1982, pp. 119-130.
15. Branson, D. E., and Trost, H., "Application of the I-Effective Method in Calculating Deflections of Partially Prestressed Members," *PCI JOURNAL*, V. 27, No. 5, Sept.-Oct. 1982, pp. 62-77.
16. Tadros, M. K., and Sulieman, H., Discussion of Ref. 13 by Branson and Trost, *PCI JOURNAL*, V. 28, No. 6, Nov.-Dec. 1983, pp. 131-136.
17. Branson, D. E., "Instantaneous and Time-Dependent Deflections of Simple and Continuous Reinforced Concrete Beams," HPR Report No. 7, Part 1, Alabama Highway Department, Bureau of Public Roads, August 1965, p. 78.
18. CEB-FIP, *Model Code for Concrete Structures*, 1978, Comité Euro-International du Béton, 6 Rue Lauriston, F-75116, Paris, France.
19. Favre, R., Beeby, A. W., Falkner, H., Koprna, M., and Schiessl, P., "Cracking and Deformation," Bulletin d'Information No. 143, Comité Euro-International du Béton, 6 Rue Lauriston, F-75116, Paris, France, Sept. 1981.
20. Trost, H., "The Calculation of Deflections of Reinforced Concrete Members - A Rational Approach," Special Publication SP-76, American Concrete Institute, Detroit, Michigan, 1982, pp. 89-108.

*Editor's Note: The third edition of the PCI Design Handbook (which will soon be published) contains essentially no changes relative to the material presented in the article on "Prestress Loss and Deflection of Precast Concrete Members."

21. Bazant, Z. P., and Oh, B. H., "Deformation of Progressively Cracking Reinforced Concrete Beams," *ACI Journal*, V. 81, May-June 1984, No. 3, pp. 268-278.
22. Tadros, M. K., Ghali, A., and Dilger, W. H., "Time-Dependent Prestress Loss and Deflection in Prestressed Concrete Members," *PCI JOURNAL*, V. 20, No. 3, May-June 1975, pp. 86-98.
23. ACI Committee 209, "Prediction of Creep, Shrinkage and Temperature Effects in Concrete Structures," Special Publication SP-76, American Concrete Institute, Detroit, Michigan, 1982, pp. 193-300.
24. Martin, L. D., "A Rational Method for Estimating Camber and Deflection of Precast Prestressed Members," *PCI JOURNAL*, V. 22, No. 1, Jan.-Feb. 1977, pp. 100-108.
25. Zia, P., Preston, H. K., Scott, N. L., and Workman, E. B., "Estimating Prestress Losses," *Concrete International*, V. 1, No. 6, June 1979, pp. 32-38.
26. Gurlitz, Carey Lang, "Loss of Prestress (Compression Loss) in Partially Prestressed Concrete," MSCE Thesis directed by F. Shaikh, Department of Civil Engineering, University of Wisconsin-Milwaukee, 1979, 135 pp.
27. AASHTO, *Standard Specifications for Highway Bridges*, American Association of State Highway and Transportation Officials, Washington, D.C., 1977.
28. Dilger, Walter H., "Creep Analysis of Prestressed Concrete Structures Using Creep Transformed Section Properties," *PCI JOURNAL*, V. 27, No. 1, Jan.-Feb. 1982, pp. 989-117.
29. Shaikh, A. F., and Branson, D. E., "Non-Tensioned Steel in Prestressed Concrete Beams," *PCI JOURNAL*, V. 15, No. 1, Jan.-Feb. 1970, pp. 14-36.
30. ACI Committee 435, "Proposed Revisions to ACI Building Code and Commentary Provisions on Deflections," *ACI Journal*, Proceedings, V. 75, No. 6, June 1978, pp. 229-238.

APPENDIX A — PRESTRESS LOSS CALCULATION

The method presented here is a simplified form of that given in Refs. 5 and 22. The Trost-Bazant aging coefficient χ is utilized in evaluating creep of concrete due to variable stress. The method is equally applicable to pretensioned and single-stage post-tensioned members, except that Step 1, which is given here for pretensioned members, can be applied to post-tensioned members only if (ES) in prestressed steel is taken equal to zero, yielding $f_{ps0} = f_{psi}$. If multistage post-tensioning is used, further adjustments would be needed.

In some of the following terms, the gross concrete section properties are used as approximations of net, or transformed section properties. This is an accepted simplification unless an unusually large amount of steel is used. The time-dependent losses given are ultimate values. When losses at an intermediate time are needed, use adjusted material properties ϵ_{sh} , C_u , C'_u , and L_r .

Step 1 — Stress Loss at Transfer

$$ES = n_i f_{cr} \quad (A1)$$

where $n_i = E_s/E_{ci}$, and f_{cr} is concrete stress at centroid of total steel area due to initial prestress and member weight.

$$f_{cr} = (P_{co}/A_g) + (P_{co} e_{ps} e_{ts}/I_g) - (M_d e_{ts}/I_g) \quad (A2)$$

Since P_{co} is yet to be determined, it is reasonable for initial calculation of ES to assume that $P_{co} = 0.9 P_i$. Initial stresses immediately after transfer are $f_{ps0} = f_{pi} - (ES)$, and $f_{s0} = -(ES)$ in the prestressed and nonprestressed steel, respectively.

Initial force in concrete, can now be calculated more accurately:

$$P_{co} = f_{ps0} A_{ps} + f_{s0} A_s \quad (A3)$$

Substituting this value of P_{co} back into Eq. (A2) results in an improved value of f_{cr} , for use in Step 3.

Step 2 — Stress Loss Due to Shrinkage

$$SH = K \epsilon_{sh} E_s \quad (A4)$$

where

$$K = 1/[1 + (E_s A_{ts}/E_{ci} A_g) \cdot (1 + e_{ts}^2/r^2)(1 + \chi C_u)] \quad (A5)$$

The symbols A_{ts} and e_{ts} are the total steel area and its eccentricity, respectively.

Step 3 — Stress Loss Due to Creep

$$CR = K [n_1 C_u f_{cr} + n(1 + C'_u) f_{cds}] \quad (A6)$$

where

f_{cds} = stress at centroid of total steel area due to superimposed dead loads not used in computing f_{cr}

$$n = E_s/E_c$$

C_u = ultimate creep coefficient for concrete at loading equal to time of release of prestressing

C'_u = ultimate creep coefficient for concrete at application of the superimposed dead loads

It is here assumed that time of application of the superimposed dead loads coincides with time of attachment of nonstructural elements. Note that the instantaneous change in stress due to application of superimposed loads is included in Eq. (A6), while the corresponding change due to initial dead load is already accounted for in Step 1.

Step 4 — Stress Loss Due to Relaxation

$$REL = -\psi KL_r \quad (A7)$$

where L_r is the intrinsic (constant length) relaxation loss.

See Ref. 3 for estimates of L_r for stress relieved and for low relaxation steel. The symbol ψ designates a factor that accounts for the reduction in relaxation loss resulting from the continual shortening of tendon embedded in concrete

due to creep and shrinkage. Values of ψ may be obtained from a chart presented in Ref. 22 or from the following formula which is a straight line approximation of that chart.

$$\psi = 1 - 3[(SH + CR)/f_{ps0}] \quad (A8)$$

Step 5 — Total Time-Dependent Loss of Compression Force in Concrete

$$\Delta P = -A_{ts}(SH + CR) - A_{ps}(REL) \quad (A9)$$

Note that the negative sign designates a tensile force increment. For lightweight concrete, appropriate values of the material properties, such as E_{cb} , E_c , ϵ_{sh} , C_u , and C'_u should be used.

For precast concrete members, Eqs. (A4) — (A7) reduce to Eq. (A10) — (A13) when the following representative parameters are adopted:

Relative humidity = 70 percent

Volume to surface ratio, $V/S = 1.5$

Concrete unit weight = 150 pcf

Accelerated curing, release strength (at concrete age 1 to 3 days)

$$f'_{ci} = 3,500 \text{ psi}$$

$$E_{ci} = 3600 \text{ ksi}, f'_c = 5000 \text{ psi}$$

$$E_c = 4300 \text{ ksi}$$

$$C_u = 1.88, C'_u = 1.50$$

$$\epsilon_{sh} = 550 \times 10^{-6}, \chi = 0.7$$

$$f_{ps0}/f_{pu} = 0.65 \text{ and } 0.7 \text{ for stress relieved}$$

METRIC (SI) CONVERSION FACTORS

$$1 \text{ ft} = 0.305 \text{ m}$$

$$1 \text{ in.} = 25.4 \text{ mm}$$

$$1 \text{ in.}^2 = 645.2 \text{ mm}^2$$

$$1 \text{ in.}^4 = 42,077 \text{ mm}^4$$

$$1 \text{ kip} = 4.45 \text{ kN}$$

$$1 \text{ plf} = 14.56 \text{ N/m}$$

$$1 \text{ ksi} = 6.9 \text{ MPa}$$

$$1 \text{ psi} = 0.0069 \text{ MPa}$$

$$1 \text{ in-kips} = 0.113 \text{ kN-m}$$

and low relaxation strands,
respectively

$L_r = -18.8$ ksi and -4.8 ksi for the two
types of strand

$E_s = E_{ps} = 28,000$ ksi, $f_{pu} = 270$ ksi

$$SH = 15.4 K \quad (A10)$$

where

$$K = 1/[1 + 18.0(A_{ts}/A_g) (1 + e_{ts}^2/r^2)] \quad (A11)$$

$$CR = K[14.6 f_{cr} + 16.3 f_{cds}] \quad (A12)$$

$$REL = 18.8 K - (4.9 + 4.7 f_{cr} + 5.2 f_{cds}) K^2 \quad (A13a)$$

or

$$REL = 4.8 K - (1.17 + 1.1 f_{cr} + 1.2 f_{cds}) K^2 \quad (A13b)$$

Eq. (13a) applies to stress relieved
strands while Eq. (A13b) applies to low
relaxation strands.

APPENDIX B — NOTATION

Sign convention — Compressive
stress in concrete and tensile stress in
steel are positive. M is positive when it
produces tension at the bottom fiber of a
member. Positive curvature corresponds
to positive M . Downward deflection is
positive.

A_g = gross area of concrete section
 A_{ps} = area of prestressed reinforcement
 A_s = area of nonprestressed tension
reinforcement
 A_{ts} = area of total steel = $A_s + A_{ps}$
 b = width of compression face of
member
 b_w = web width
 C = creep coefficient, defined as
creep strain divided by initial
strain due to constant sustained
stress
 C_a = creep coefficient for age of load-
ing at release and loading dura-
tion up to time of erection
 C_u = ultimate creep coefficient for
concrete at loading equal to
time of release of prestressing
 C'_u = ultimate creep coefficient for
loading at time of attachment
of nonstructural elements, as-
sumed to occur at time of super-
imposed dead load application
 CR = stress loss due to creep of con-
crete

d = distance from extreme compres-
sion fiber to centroid of tension
reinforcement
 d_{ps} = distance from extreme compres-
sion fiber to centroid of pre-
stressing steel
 e_c = eccentricity of prestress force
from centroid of section at cen-
ter of span
 e_{cr} = eccentricity of prestress force
from centroid of cracked section
 e_e = eccentricity of prestress force
from centroid of section at end
of span
 e_{ps} = eccentricity of prestressed steel
measured from centroid of un-
cracked section
 e_{ts} = eccentricity of total steel area
measured from centroid of un-
cracked section
 E_c = modulus of elasticity of con-
crete at service
 E_{ct} = modulus of elasticity of con-
crete at time of initial prestress
 E_s = modulus of elasticity of steel
 ES = stress loss due to elastic short-
ening of concrete
 f_{cds} = concrete compressive stress at
center of gravity of $A_s + A_{ps}$ due
to all permanent (dead) loads
not used in computing f_{cr}
 f_{cr} = concrete stress at center of grav-
ity of combined steel immedi-
ately after transfer

f_{pst}	= stress in prestressed reinforcement immediately prior to release	P_{co}	= prestress force in concrete, immediately after release
f_{ps}	= stress in prestressed reinforcement immediately after release	P_i	= prestress force before release
f_r	= modulus of rupture of concrete	ΔP_c	= time-dependent loss of compressive prestress force in concrete, assumed, to be applied at centroid of combined steel area
f_{so}	= stress in nonprestressed steel immediately after release	R	= $(M_{cr} - M_o)/(M_a - M_o)$, see Eqs. (4) and (5)
f_{tm}	= apparent tensile stress at extreme bottom fiber due to total load moment and effective prestress using uncracked section properties	r	= radius of gyration = $\sqrt{I_o/A_o}$
h_f	= depth of flange	REL	= stress loss due to relaxation of tendons
I_{cr}	= moment of inertia of cracked section transformed to concrete	SH	= stress loss due to shrinkage of concrete
I'_e	= effective moment of inertia for computation of curvature at a section	y_{cr}	= distance from extreme compression fibers to centroid of cracked section
I_g	= moment of inertia of gross section	y_e	= effective distance from extreme compression fibers to centroid of cracked section, for curvature calculation; see Eq. (7)
K	= coefficient defined by Eq. (A5)	y_o	= distance from extreme compression fibers to centroid of uncracked section
l	= span length	α_a	= ratio of prestress loss in concrete at erection to final prestress loss
L_r	= intrinsic relaxation stress loss, for a condition of constant strain	δ	= midspan deflection or camber
M_a	= total moment at section	ϕ_c	= curvature at midspan section
M_{cr}	= cracking moment	ϕ_{cr}	= curvature at cracked section
M_o	= decompression bending moment	ϕ_e	= curvature at end section
M_d	= moment due to member weight dead load	χ	= aging coefficient
M_l	= moment due to service live load	ϵ_{sh}	= free shrinkage of concrete
M_{sl}	= moment due to superimposed dead load	ρ	= $A_{ts}/(bd)$, to be used in Figs. 1 and 2
n	= modular ratio E_s/E_c	ψ	= relaxation reduction factor, Eq. (A8)
n_t	= modular ratio E_s/E_{ct}		
P_{ce}	= effective prestress force in concrete		

* * *

NOTE: Discussion of this paper is invited. Please submit your comments to PCI Headquarters by September 1, 1985.